

# Modeling of magnetospheric chorus wave generation with 2D TRISTAN-MP PIC code

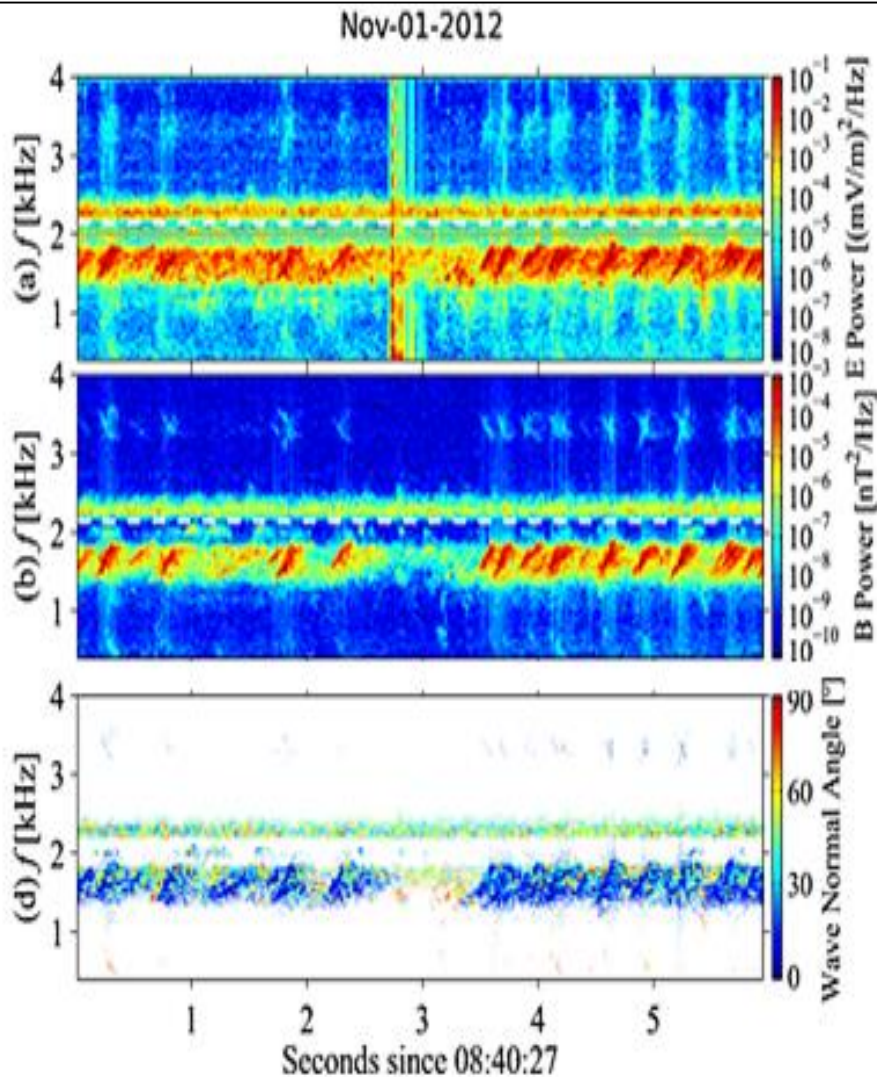
I.V. Kuzichev<sup>1</sup>, A.R. Soto-Chavez<sup>1</sup>, J. Park<sup>2,3</sup>, A. Gerrard<sup>1</sup>, A. Spitkovsky<sup>3</sup>

<sup>1</sup>New Jersey Institute of Technology, CSTR, Newark, NJ, USA

<sup>2</sup>Lawrence Berkeley National Lab, Berkeley, USA

<sup>3</sup>Department of Astrophysical Sciences, Princeton University, Princeton, USA

# Chorus waves: observations



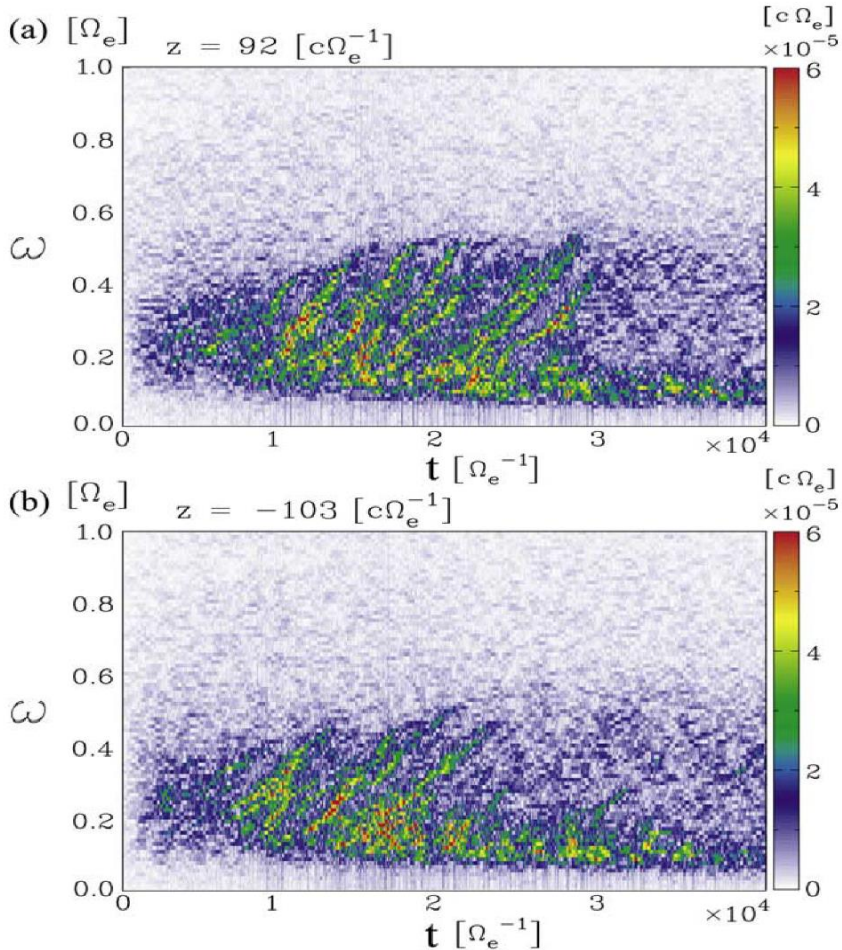
Chorus waves are one of the most important and interesting wave phenomena in the Earth's outer radiation belt. They belong to the whistler mode and have frequencies from hundreds of Hz to several kHz. They are observed as discrete series of wave packets each having varying frequency mostly in the form of rising tones, but falling tones are also found.

The study of generation mechanisms of rising<sup>1,2</sup> and, especially, falling tone chorus waves<sup>3</sup> remains an active area of research. A common feature of most of the chorus theoretical models is that they are non-linear, which significantly reduces the opportunities to investigate corresponding processes analytically. This study shows the results of chorus wave simulation with Tristan-MP 2D Particle-In-Cell (PIC) code<sup>4</sup>, which treats both cold and hot electrons kinetically and uses correct relativistic form of the distribution function.

1. Trakhtengerts, V. Y. (1995), JGR, doi:10.1029/95JA00843
2. Omura, Y., Katoh, Y. and Summers, D. (2008), JGR, doi: 10.1029/2007JA012622
3. Soto-Chavez, A. R., Wang, G., Bhattacharjee, A., Fu, G. Y. and Smith, H. M. (2014), GRL, doi: 10.1002/2014GL059320
4. Spitkovsky, A. (2005), AIP Conf. Proc., doi: 10.1063/1.2141897

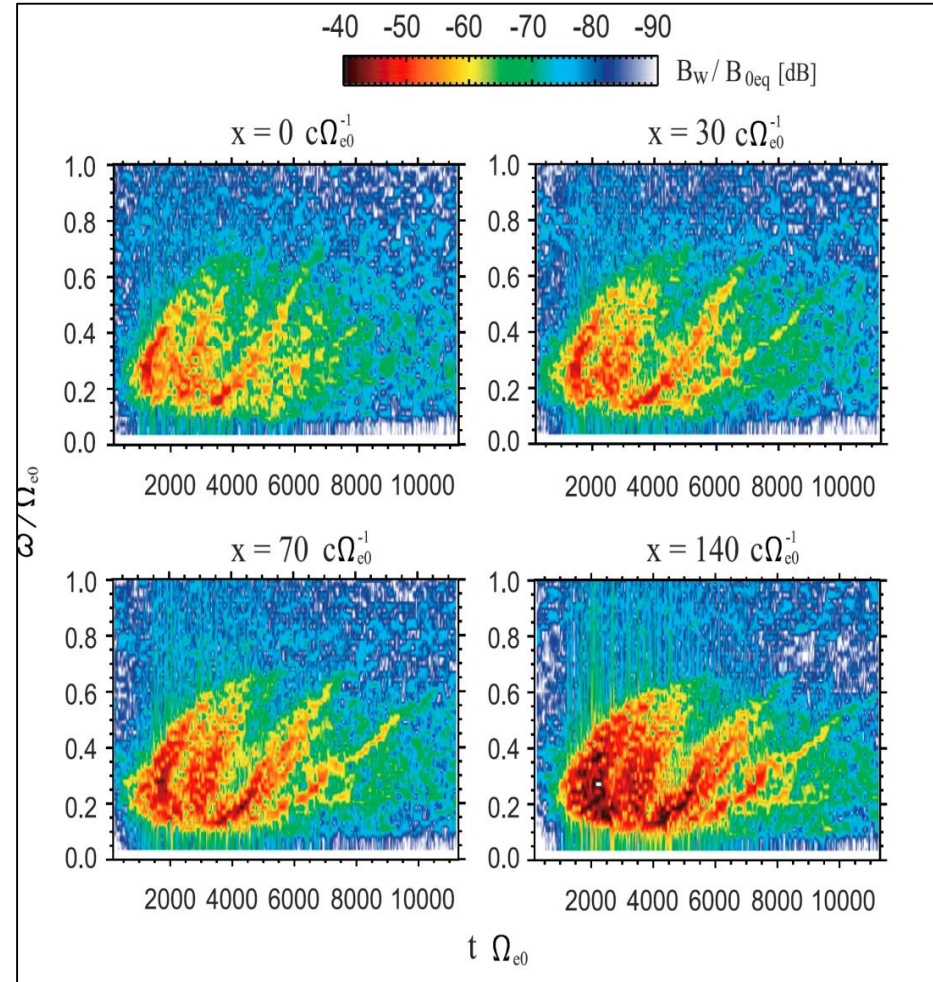
# 1D Numerical modeling of chorus waves

## Hybrid code



*Katoh, Y., and Y. Omura (2007), GRL.*

## Full PIC code



*Hikishima, M., S. Yagitani, Y. Omura, and I. Nagano (2009), JGR*

# TRISTAN-MP code

- This code is 3D fully relativistic PIC code. It was written by Buneman (1993), and developed further by, in particular, A. Spitkovsky (A. Spitkovsky, (2005) AIP Conference Proceedings).
- Code uses 2<sup>nd</sup> order FDTD scheme for EM field (Yee (1966) IEEE Transactions on Antennas and Propagation), and Boris/Vay scheme for particle mover (Boris (1970), in: Proceedings of the Fourth Conference on Numerical Simulation Plasmas; Vay (2008) Phys. Plasmas)
- Code was successfully used for simulations of relativistic shocks in astrophysical plasma

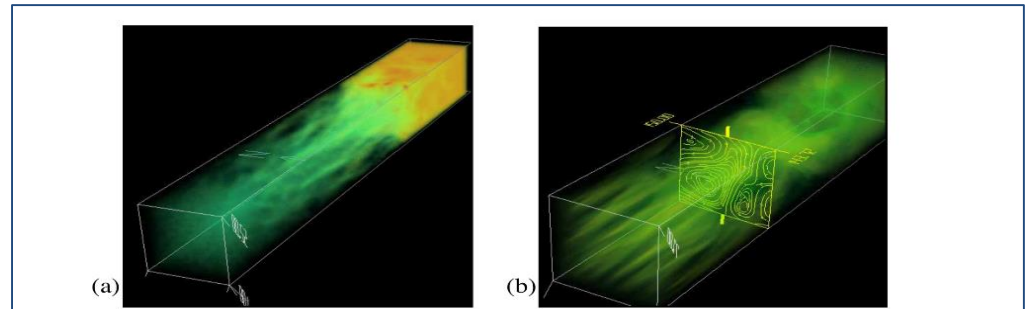


FIGURE 1. a) Filamentary structure of density in an unmagnetized shock. b) Generation of magnetic field around current filaments in the shock.

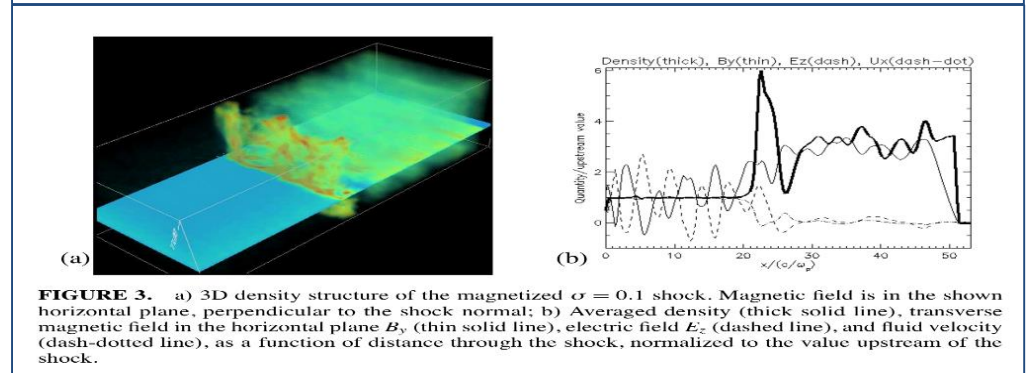


FIGURE 3. a) 3D density structure of the magnetized  $\alpha = 0.1$  shock. Magnetic field is in the shown horizontal plane, perpendicular to the shock normal; b) Averaged density (thick solid line), transverse magnetic field in the horizontal plane  $B_y$  (thin solid line), electric field  $E_z$  (dashed line), and fluid velocity (dash-dotted line), as a function of distance through the shock, normalized to the value upstream of the shock.

A. Spitkovsky, (2005) AIP Conference Proceedings

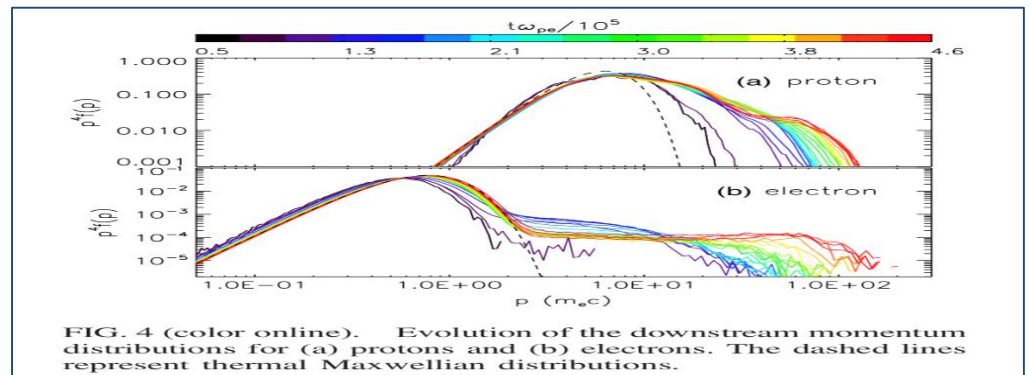


FIG. 4 (color online). Evolution of the downstream momentum distributions for (a) protons and (b) electrons. The dashed lines represent thermal Maxwellian distributions.

Park et al., (2015) PRL

# Computational resources

- The simulations were performed on CISL supercomputer in Cheyenne. One simulation for the time interval about  $2000 [1/\omega_{ce}]$  and number of particles about  $4 \cdot 10^8$  takes 6 hours on 360 cores.
- We also used NJIT Kong cluster for test runs. On this cluster, one simulation takes about 4 days on 150 cores.

Cheyenne is a 5.34-petaflops, high-performance computer built for NCAR by SGI. The system was released for production work on January 12, 2017.

An SGI ICE XA Cluster, the Cheyenne supercomputer features 145,152 latest-generation Intel Xeon processor cores in 4,032 dual-socket nodes (36 cores/node) and 313 TB of total memory.



Cheyenne's login nodes give users access to the [GLADE](#) shared-disk resource and the [High Performance Storage System](#)

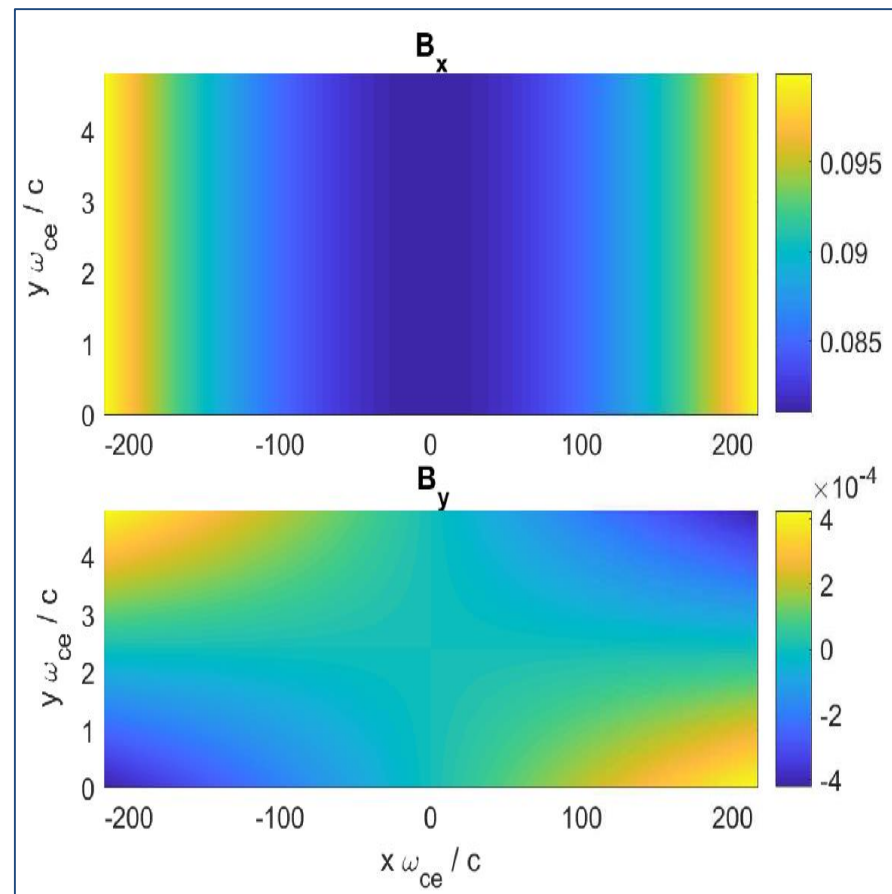
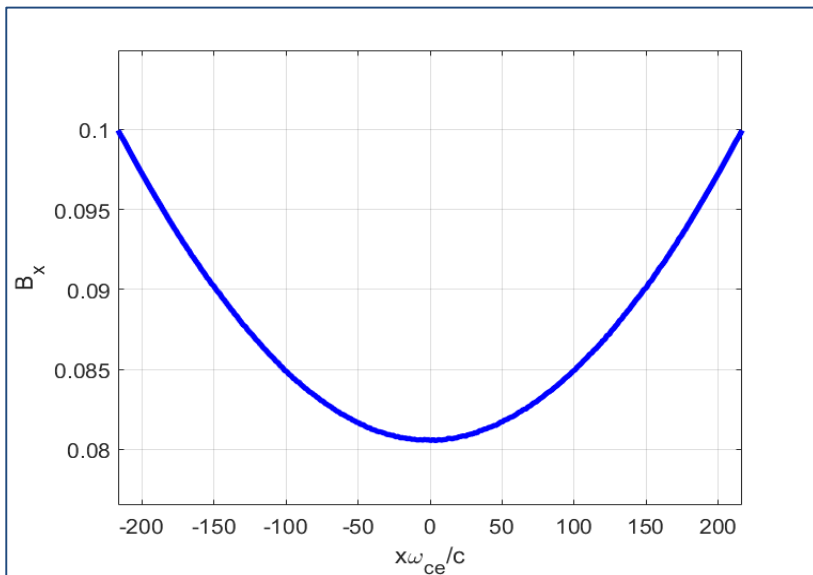


# TRISTAN-MP code: background magnetic field

We consider 2D problem with parabolic magnetic field

$$B_x = B_0 \left( 1 + \alpha (x - x_{eq})^2 \right)$$

$$B_y = -2B_0 \alpha (x - x_{eq})(y - y_0)$$



# TRISTAN-MP code: Initial distributions

Electrons are represented by two populations: cold electrons with isotropic Maxwellian distribution, and hot electrons with adiabatic anisotropic bi-Maxweillian distribution:

$$F(\vec{p}, \vec{r}) = N \exp \left\{ -\frac{mc^2}{T} \sqrt{1 + \frac{p_{\parallel}^2}{m^2 c^2 \sin^2 \delta} + \frac{p_{\perp}^2 h(\vec{r})}{m^2 c^2 \cos^2 \delta}} \right\}$$

$$h(\vec{r}) = 1 + (ctg^2 \delta - 1) \left( 1 - \frac{B_0}{B(\vec{r})} \right)$$

The main parameters are:

$$T = 100 \text{ keV}, \delta = 0.4,$$

$$p_{T\parallel} = 0.17mc (15 \text{ keV})$$

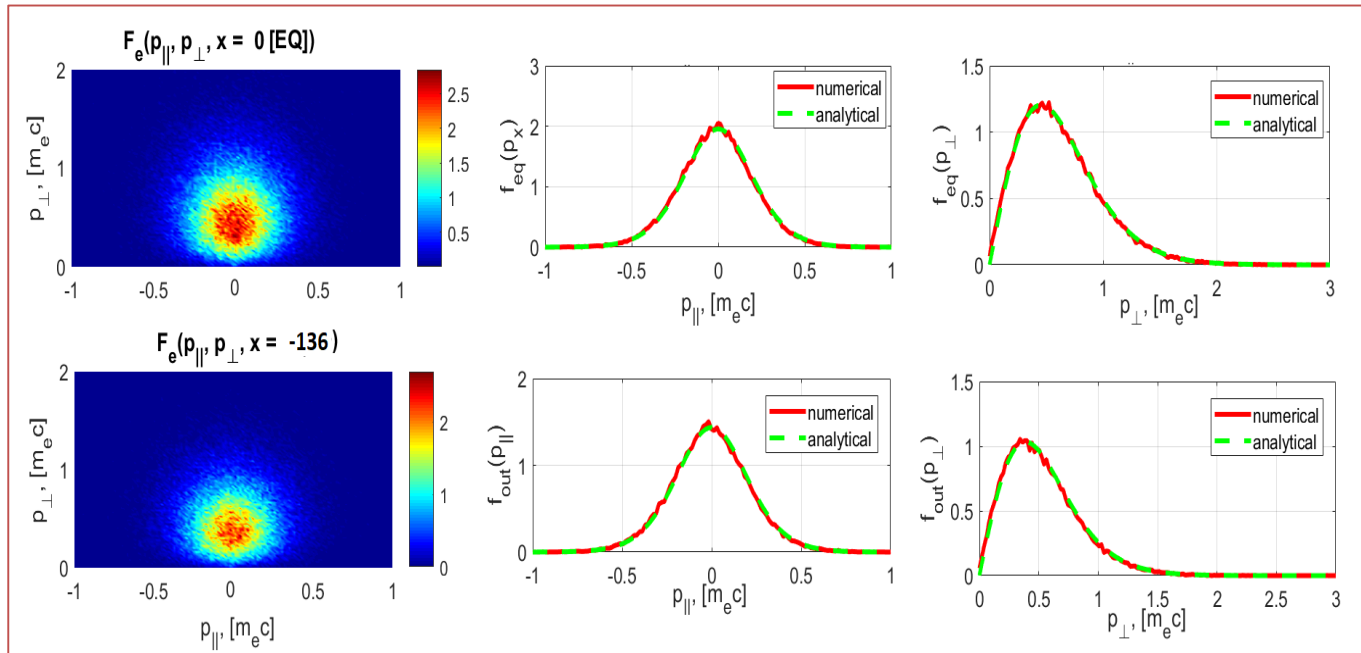
$$p_{T\perp} = 0.41mc (85 \text{ keV})$$

$$A = \frac{T_{\perp}}{T_{\parallel}} - 1 \approx 4.7$$

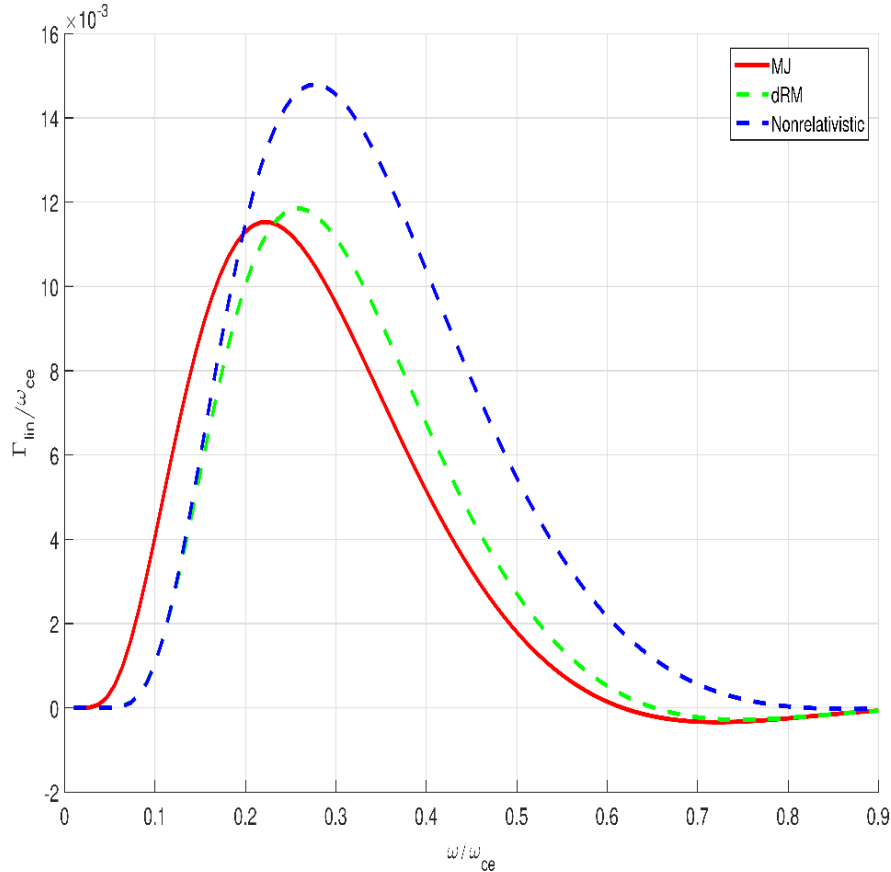
$$\alpha = 0.5 \cdot 10^{-5} \omega_{ce}^2 / c^2$$

Cell = 1080x10,

Particles per Cell =  $2 \cdot 10^4$



# Linear increment: importance of MJ form of distribution



We use relativistic bi-Maxwellian derived from Maxwell-Juttner distribution

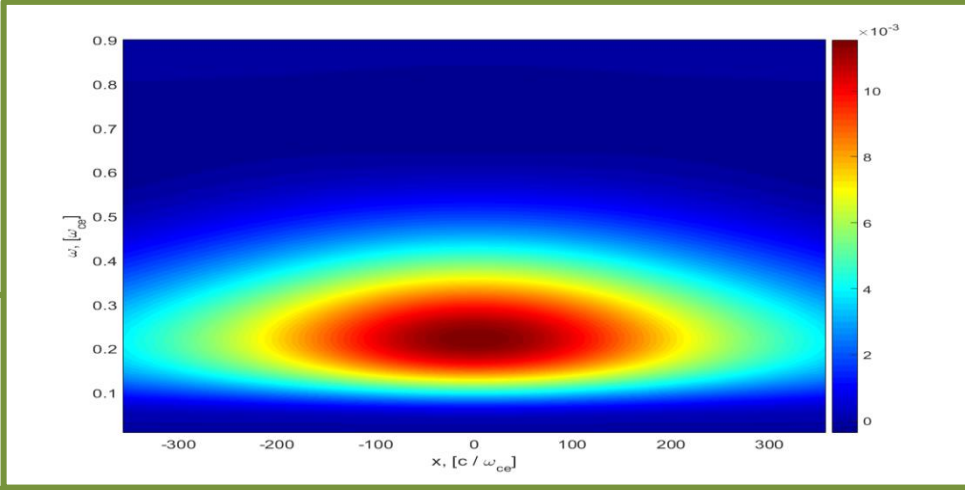
$$F(\vec{p}) = Ne^{-\frac{1}{T} \sqrt{1 + \frac{p_{\parallel}^2}{\sin^2(\delta)} + \frac{p_{\perp}^2}{\cos^2(\delta)}}$$

Previously, direct relativistic expansion of non-relativistic bi-Maxwellian was used in the most simulations (Hikishima et al. (2009), JGR.; Tao, X. (2014), JGR)

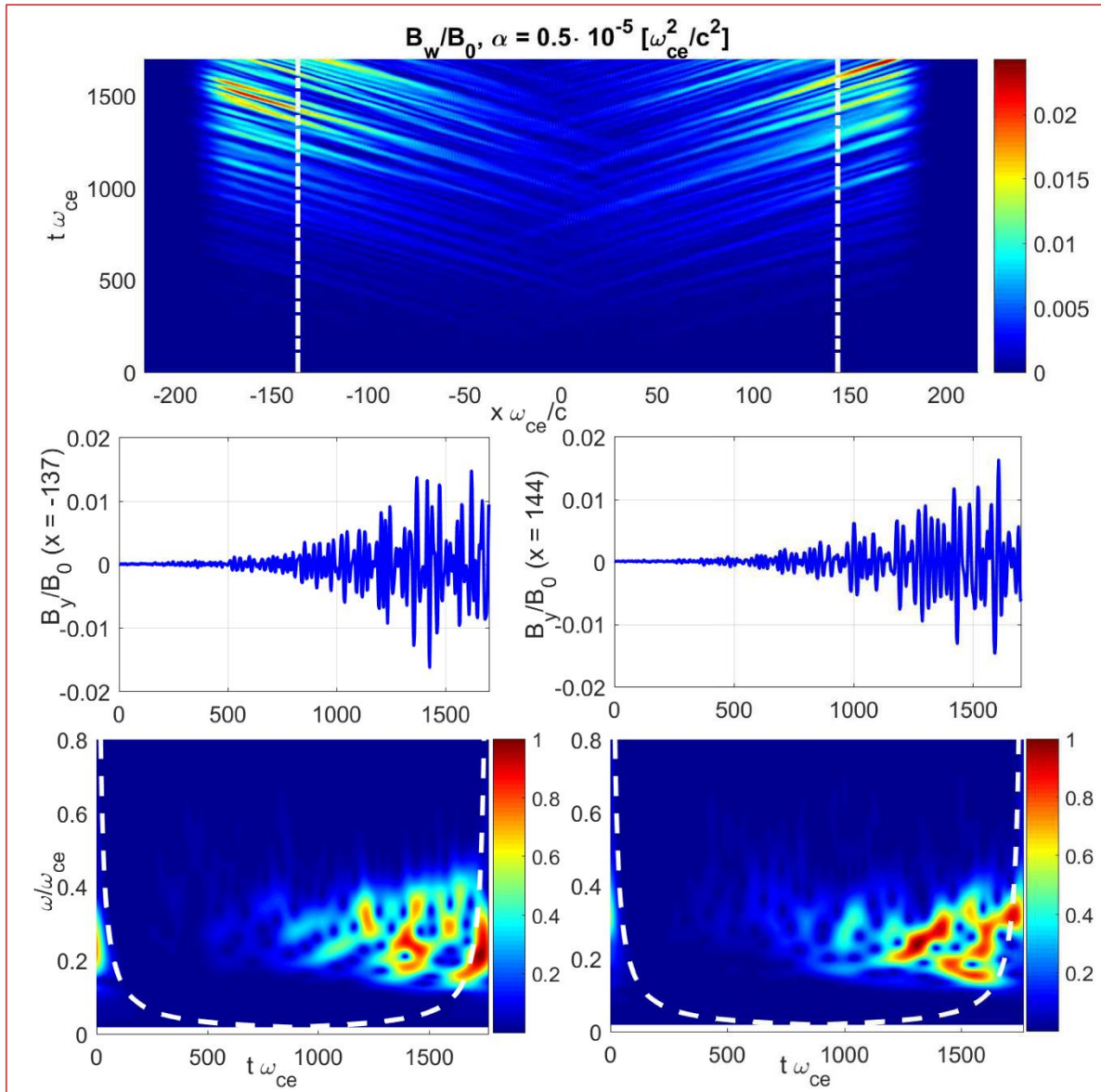
$$F(\vec{p}) = Ne^{-\frac{p_{\parallel}^2}{2T_{\parallel}} - \frac{p_{\perp}^2}{2T_{\perp}}}$$

$T = 100$  [keV]  
 $\delta = 0.4$

Taking spatial inhomogeneity into account



# Wave generation



The waves are generated in the equatorial region and propagate from the equator, being amplified.

Temporal behavior of the wave field at spatial points, indicated by white lines

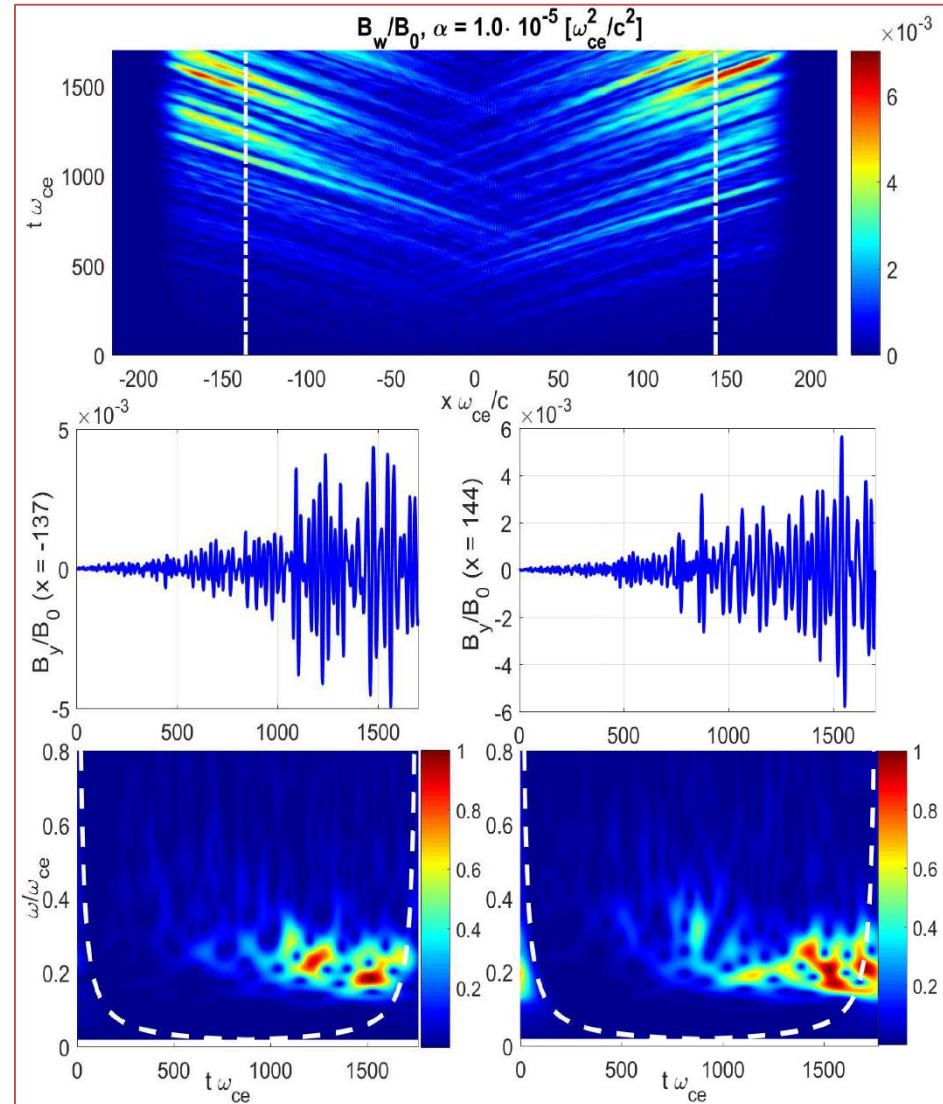
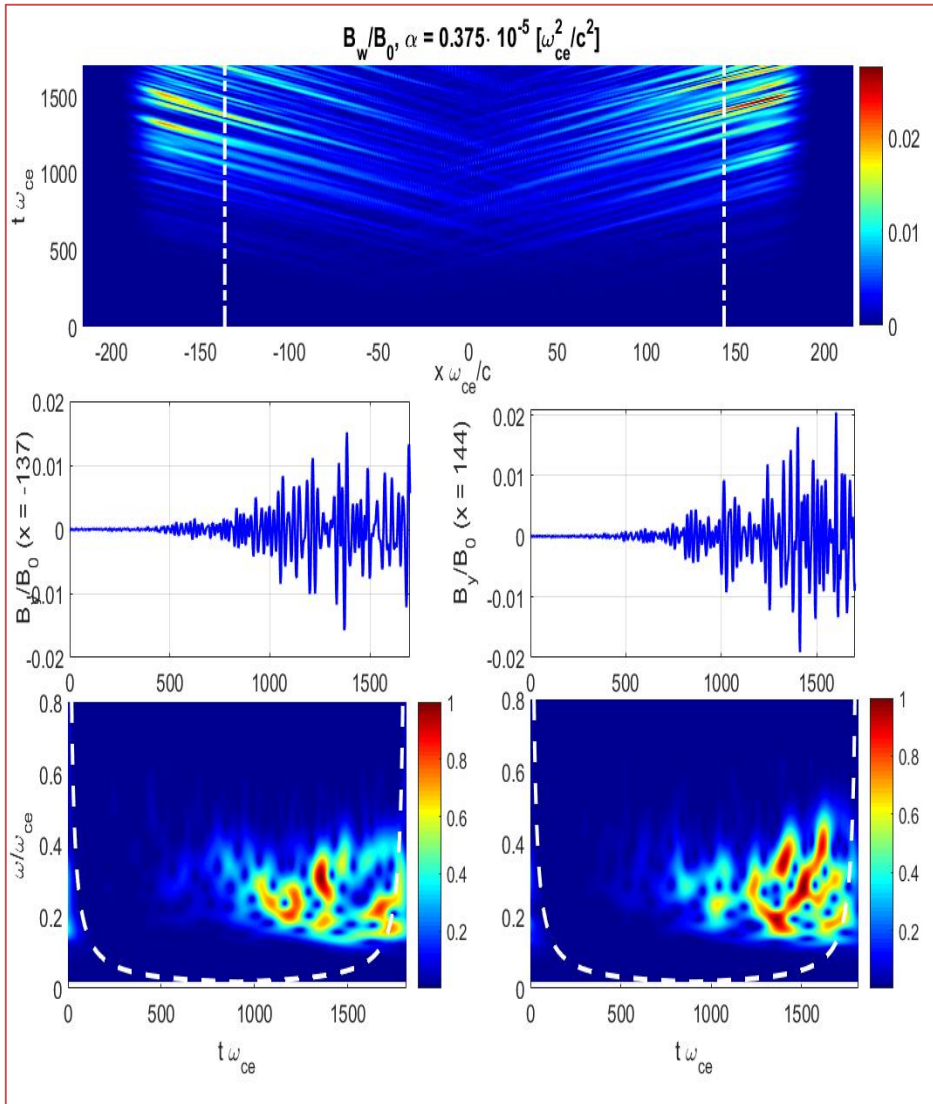
Temporal-spectral analysis of the signal. Rising tone chorus-like elements are generated to the right from the equator.

# Changing the inhomogeneity $\alpha$

$$B_x = B_0 \left( 1 + \alpha (x - x_{eq})^2 \right)$$

Smaller inhomogeneity: rising tone remains

Higher inhomogeneity: no clear chirping



# Frequency chirping rate

Inhomogeneity increases

$$\alpha = 0.125 \cdot 10^{-5} [\omega_{ce}^2/c^2]$$

$$\partial\omega/\partial t \sim 14 \cdot 10^{-4} [\omega_{ce}^{-2}]$$

$$\alpha = 0.375 \cdot 10^{-5} [\omega_{ce}^2/c^2]$$

$$\partial\omega/\partial t \sim 8 \cdot 10^{-4} [\omega_{ce}^{-2}]$$

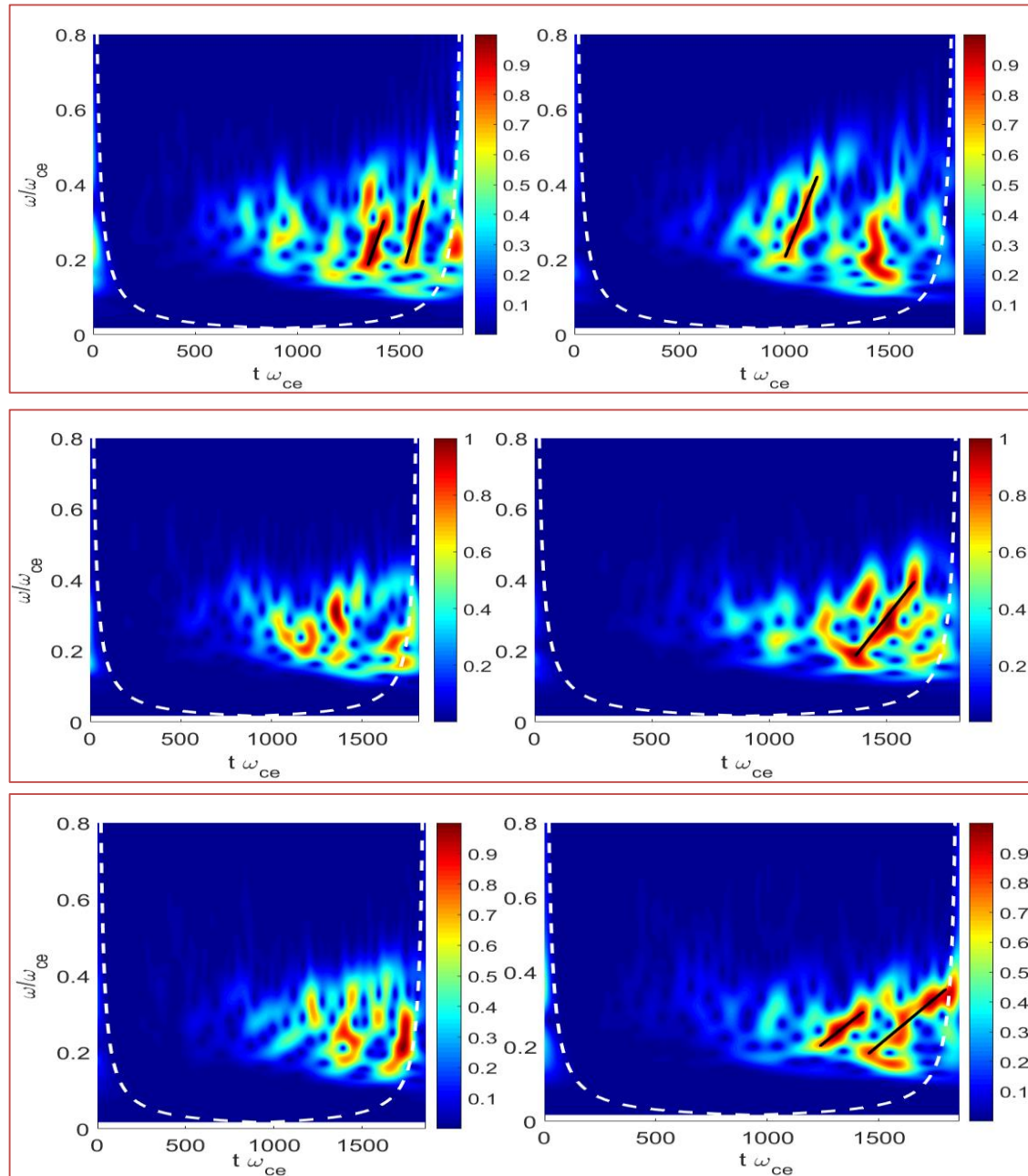
$$\alpha = 0.5 \cdot 10^{-5} [\omega_{ce}^2/c^2]$$

$$\partial\omega/\partial t \sim 4 \cdot 10^{-4} [\omega_{ce}^{-2}]$$

Chirping rate decreases

$$x = -137 [c/\omega_{ce}]$$

$$x = 144 [c/\omega_{ce}]$$



# Theoretical prediction

$$\frac{\partial \omega}{\partial t} = \frac{0.4\delta}{\gamma \xi} \frac{V_{\perp 0}}{c} \frac{\omega}{\Omega_e} \left(1 - \frac{V_R}{V_g}\right)^{-2} \left(\frac{B_w}{B_0}\right) \Omega_e^2$$

Omura et al., (2008), JGR

Inhomogeneity increases

$$\alpha = 0.125 \cdot 10^{-5} [\omega_{ce}^2/c^2]$$

$$\partial \omega / \partial t \sim 14 \cdot 10^{-4} [\omega_{ce}^{-2}]$$

$$\langle B_w/B_0 \rangle \approx 0.012$$

Chirping rate decreases

$$\alpha = 0.375 \cdot 10^{-5} [\omega_{ce}^2/c^2]$$

$$\partial \omega / \partial t \sim 8 \cdot 10^{-4} [\omega_{ce}^{-2}]$$

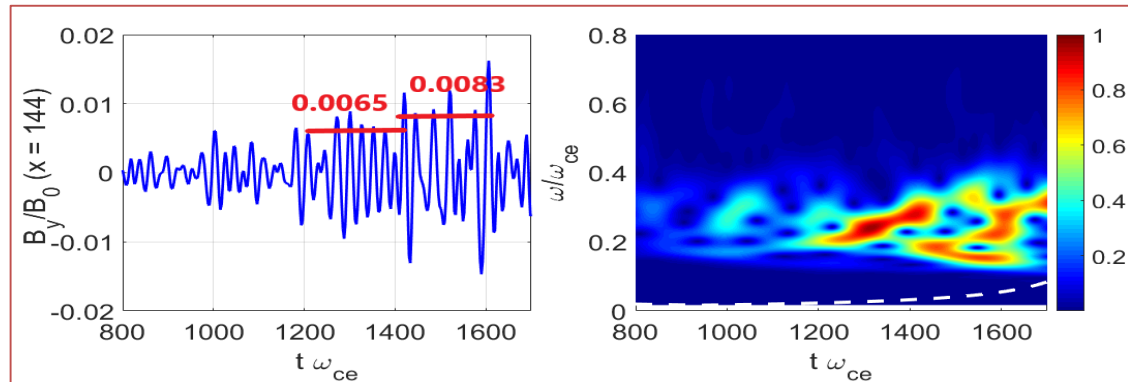
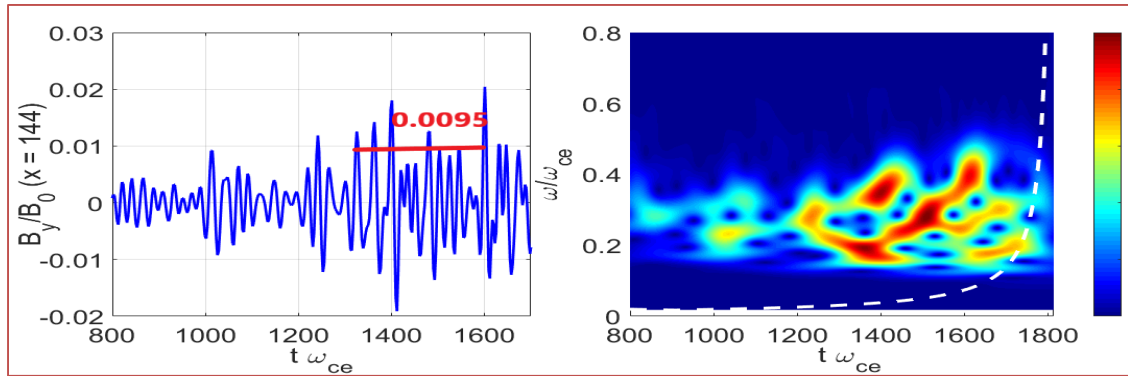
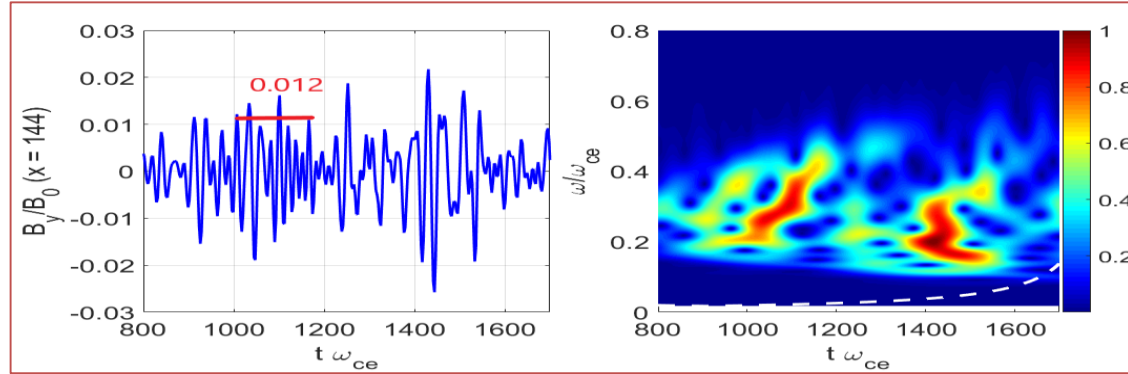
$$\langle B_w/B_0 \rangle \approx 0.0095$$

$$\alpha = 0.5 \cdot 10^{-5} [\omega_{ce}^2/c^2]$$

$$\partial \omega / \partial t \sim 4 \cdot 10^{-4} [\omega_{ce}^{-2}]$$

$$\langle B_w/B_0 \rangle \approx 0.0065$$

$$\langle B_w/B_0 \rangle \approx 0.0083$$



# Summary

- We successfully generated rising tone chorus-like waves using 2D full PIC code TRISTAN-MP
- Higher inhomogeneity suppresses wave generation in agreement with theoretical predictions and 1D simulations
- Chirping rate seems to be decreasing with inhomogeneity
- Asymmetry of wave generation with respect to the equator is observed.

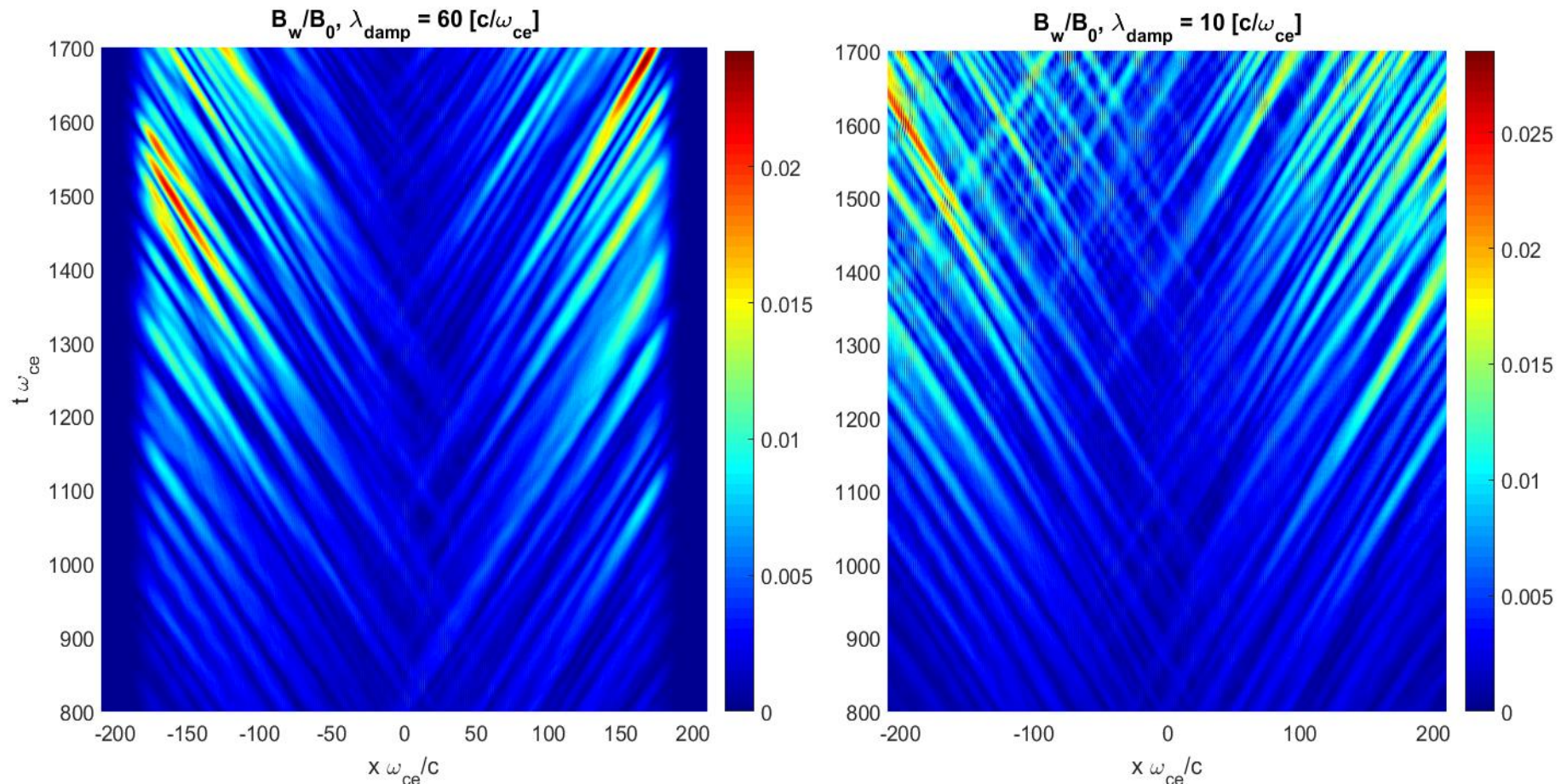
# Further plans

- Study the generation and properties of oblique chorus waves
- Investigate the evolution of electron distribution function: does electromagnetic hole associated with chorus wave in 1D exist and stable in 2D?
- Study numerically the predictions of theory (Soto-Chavez et al. (2014) GRL) that falling-tone chorus waves might be excited due to the competition between Landau and first cyclotron resonance

Thank you!

# TRISTAN-MP code: absorbing boundaries

To avoid spurious reflection of the waves from the boundaries, we implement an absorbing mask modifying the Maxwell's at distances  $< \lambda$  from the boundaries. The distance is chosen empirically.



# TRISTAN-MP code: particle sampling

Due to code parallel architecture, we use different methods to obtain correct momentum distribution and spatial adiabatic distribution

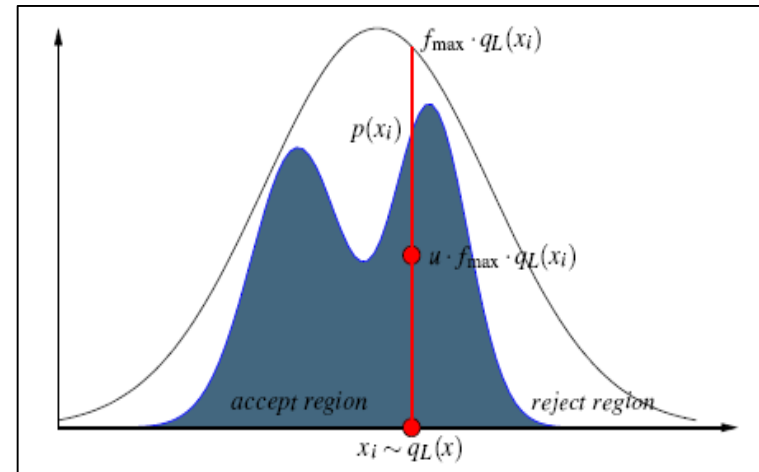
$$F(\vec{p}, \vec{r}) = N \exp \left\{ -\frac{mc^2}{T} \sqrt{1 + \frac{p_{\parallel}^2}{m^2 c^2 \sin^2 \delta} + \frac{p_{\perp}^2 h(\vec{r})}{m^2 c^2 \cos^2 \delta}} \right\}$$

$$h(\vec{r}) = 1 + (ctg^2 \delta - 1) \left( 1 - \frac{B_0}{B(\vec{r})} \right)$$

## Momentum distribution: inverse transform method

1. Given the probability density function  $f(E)$ , we calculate cumulative probability function  $P(E) = \int f(E) dE$ ,  $P(E) \in [0, 1]$ . Here,  $E$  is the energy of the particle
2. Using random number generator with the uniform distribution on  $[0, 1]$ , we generate random number  $\eta$ .
3. Now, we assign for the particle the corresponding value of  $E$ :  $\eta = P(E)$ .
4. To account for anisotropy, rescale the dispersion for energy  $E$  accordingly.
5. Proceed to the next particle.

## X-distribution: rejection sampling



$u \sim \text{uniform } [0, 1]$

$q_L(x)$  – any distribution we can sample from

$p(x)$  – distribution we need to obtain